Optical Multi-Path Interference Noise Mitigation for 56 Gb/s PAM4 IMDD Transmission System

Chuanming Huang, Haiping Song, Mengfan Cheng, Qi Yang, Ming Tang, Deming Liu, Lei Deng*
School of Optical and Electronic Information, Huazhong University of Science and Technology, Wuhan 430074, China
*denglei_hust@mail.hust.edu.cn

Abstract: We experimentally demonstrate two multi-path-interference (MPI) mitigation algorithms that can effectively suppress the MPI noise in 56Gb/s PAM4 signal transmission over 15.5km SSMF system, under the signal-to-interference ratio of 18dB and laser linewidth of 4MHz.
OCIS codes: (060.2330) Fiber optics communication; (060.4080) Modulation; (060.4510) Optical communications

1. Introduction

Intensity modulation direct detection (IMDD) is a promising solution for short-reach fiber optics communication, such as datacenter and PON, due to its low complexity and low cost [1]. Moreover, the PAM4 modulation format has been an attractive way to increase the spectral efficiency in the IMDD system and it has been widely investigated and experimentally demonstrated [2]. However, it is well known that the PAM4 signal is highly vulnerable to optical multipath interference (MPI) noise, which is caused by multiple reflections from dirty fiber connectors. It is believed that the MPI noise is the main limitation in the practical application of the PAM4 modulation format [3]. To solve this problem, high-frequency phase modulation is introduced in [4] for MPI noise suppression, and the fundamental mechanism of this scheme is the redistribution of noise energy to high frequencies. This scheme needs to modify the existing IMDD system architecture, which is not compatible with the existing fiber optics communication system. In [5], a high-pass filter (HPF) is introduced at the receiver to mitigate the MPI noise which is considered as the low-frequency noise, and the HPF cut-off frequency is adjusted by changing the capacitance of the DC blocking capacitor of the receiver in the experiment. However, the received signal may be degraded by the HPF while the MPI noise is not serious, and the HPF scheme is ineffective for larger laser linewidth. Besides, the HPF may produce the baseline-wandering effect which hurts the received signal [6]. In [7], an error signal is generated through the MPI impaired signal and its corresponding decision PAM level, and this error signal is filtered by a low-pass filter to estimate the MPI noise. The estimated noise is then subtracted from the MPI impaired signal. This work only proposes the concept, and no experiment has been demonstrated. In general, a scheme that can effectively mitigate the MPI noise without affecting the transmission performance or changing the existing transmission system architecture is highly desired.

In this paper, we propose and experimentally demonstrate two kinds of algorithms that can effectively suppress the MPI noise in a high-speed PAM4 IMDD transmission system. The first algorithm utilizes the fluctuation characteristic in MPI impaired PAM4 signals, and the fluctuation caused by MPI noise could be suppressed by removing the instantaneous intensity offset of the fluctuating PAM4 signals. The second algorithm utilizes the intensity-dependent characteristic of MPI noise, and the MPI noise is suppressed by subtracting the reconstructed MPI noise, which is multiplied by a weighting factor related to the PAM level, from the MPI impaired PAM4 signals. With the help of these two MPI noise mitigation algorithms, 56 Gb/s PAM4 signals could be successfully transmitted over 15.5 km standard single-mode fiber (SSMF) under the signal-to-interference ratio (SIR) of 18 dB, and the laser linewidth tolerance can reach 4 MHz. This indicates that the proposed MPI noise mitigation algorithms are still effective for large laser linewidth compared to the HPF scheme.

2. Principle

The schematic diagram of the MPI generation is shown in Fig. 1(a). Obviously, the MPI noise is the accumulation of many reflected signals. For the sake of simplicity, we assume that the MPI impaired optical signal can be approximated as the combination of a direct signal and a doubly reflected signal, and the received signal at the receiver can be expressed as

$$\begin{cases} \mathrm{E}_{out}(\mathrm{t}) = \mathrm{E}_s(\mathrm{t})\,\mathrm{e}^{j\phi(\mathrm{t})} + \alpha\,\mathrm{E}_s(\mathrm{t}-\tau)\,\mathrm{e}^{j\phi(\mathrm{t}-\tau)} \\ \mathrm{I}_{PD}(\mathrm{t}) = \left|\mathrm{E}_{out}(\mathrm{t})\right|^2 = \left|\mathrm{E}_s(\mathrm{t})\right|^2 + \left|\alpha\,\mathrm{E}_s(\mathrm{t}-\tau)\right|^2 + 2\alpha\,\mathrm{Re}[\mathrm{E}_s^*(\mathrm{t})\,\mathrm{E}_s(\mathrm{t}-\tau)]\cos[\phi(\mathrm{t})-\phi(\mathrm{t}-\tau)] \end{cases}, \tag{1}$$

where $\mathrm{E}_s(\mathrm{t})$ is the optical signal, $\phi(\mathrm{t})$ is the phase noise, and α is the loss factor of the reflected signal. τ is the time delay of the reflected signal relative to the direct signal, $\mathrm{I}_{PD}(\mathrm{t})$ is the detected signal while the response of photodetector (PD) is assumed to be 1. The simulated MPI impaired PAM4 signal is shown in Fig. 1(b). It can be

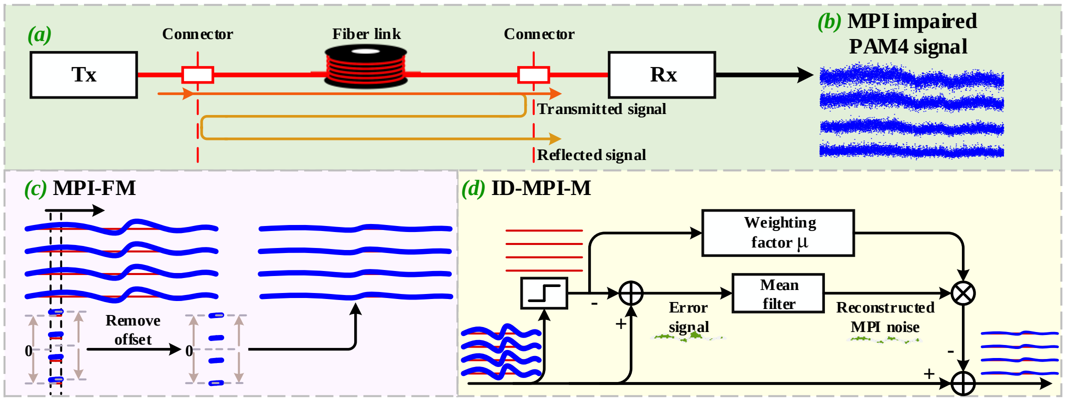

Fig. 1. (a) The schematic diagram of the MPI noise generation, (b) the simulated MPI impaired PAM4 signal, (c-d) the schematic diagram of the proposed two MPI mitigation algorithms.

seen that the MPI impaired PAM4 signal shows the characteristic of irregular fluctuation, and the higher PAM level suffers worse, which shows the intensity-dependent characteristic of MPI noise.

According to the characteristic of MPI noise, we propose two MPI suppression methods. The first MPI suppression method utilizes the fluctuation characteristic of MPI impaired PAM4 signal, and the schematic diagram is shown in Fig. 1(c). Obviously, there has an instantaneous intensity offset in the MPI impaired PAM4 signal. Therefore, we can smooth out the fluctuation of MPI impaired PAM4 signal by removing the offset value, which is denoted as MPI-fluctuation-mitigation (MPI-FM) algorithm and can be expressed as

$$\mathrm{R1(n)} = \mathrm{R(n)} - \frac{1}{N}\sum_{i=n-N/2+1}^{n+N/2} \mathrm{R(i)}, \tag{2}$$

where R(n) is the MPI impaired PAM4 signal and n is the data index. N is the symbol length that needs to be optimized and R1(n) is the output signal. The second MPI suppression method utilizes the intensity-dependent characteristic of MPI noise, and the schematic diagram is shown in Fig. 1(d). The MPI noise is firstly reconstructed by averaging the error signal, which is the difference of the MPI impaired PAM4 signal minus the corresponding decision PAM4 signal. According to the intensity-dependent characteristic of MPI noise, the reconstructed MPI noise is then multiplied by a weighting factor related to the decision PAM signal and subtracted from the MPI impaired signal to suppress MPI noise. This MPI suppression method is denoted as intensity-dependent MPI mitigation (ID-MPI-M) algorithm and it can be described as

$$\begin{cases} \mathrm{MPI(n)} = \dfrac{1}{N}\displaystyle\sum_{i=n-N/2+1}^{n+N/2} [\mathrm{R(i)} - \mathrm{R_d(i)}] \\ \mathrm{R1(n)} = \mathrm{R(n)} - \mu_n \,\mathrm{MPI(n)} \end{cases}, \tag{3}$$

where $\mathrm{R_d}(\cdot)$ is the decision value of $\mathrm{R}(\cdot)$, μ_n is the weighting factor which depends on the decision result of R(n).

3. Experimental setup and results

Fig. 2 shows the experimental setup of an MPI impaired IMDD PAM4 system. At the transmitter, pseudorandom bit sequences (PRBS) are generated and then mapped into a PAM4 format signal with a bit rate of 56 Gb/s. The generated PAM4 signal is up-sampled by a factor of 2 and then is filtered by a root-raised cosine (RRC) filter, whose roll-off factor R is 0.1. The produced PAM4 signal is load into an arbitrary waveform generator (AWG, Keysight M8195A) with a sampling rate of 64 GSa/s. The output signal of AWG with a peak-to-peak voltage of 130mv is amplified by an electrical amplifier (EA, Centellax OA3MHQM4), and then it is used to drive a Mach-Zehnder modulator (MZM). A continuous-wave (CW) laser with an optical power of 15.5 dBm is used as the optical source. The wavelength and linewidth of the CW laser are 1550 nm and 100 kHz, respectively. Besides, another DFB laser with a linewidth of 4 MHz is used for comparison. To simulate the impact of MPI, the output of MZM is split into two branches. The signal in the upper branch is transmitted 15.5 km SSMF and works as the transmitted signal. The signal in the lower branch is transmitted 2.8 km SSMF and works as the reflected signal. The polarization state of the reflected signal is adjusted by a polarization controller (PC). A variable optical attenuator (VOA1) is used to adjust the intensity of the reflected signal, and thus the signal-to-interference ratio (SIR) can be adjusted. The transmitted signal and reflected signal are combined by an optical coupler and then detected by a PD. The VOA2 is used to adjust the received optical power (ROP). The detected electrical signal is finally captured by a digital sampling oscilloscope (DSO, Tektronix DPO 73304D) with a sampling rate of 100 GSa/s for the offline process in Rx DSP. The MPI-FM and ID-MPI-M algorithms are used to suppress the MPI noise and an HPF with a

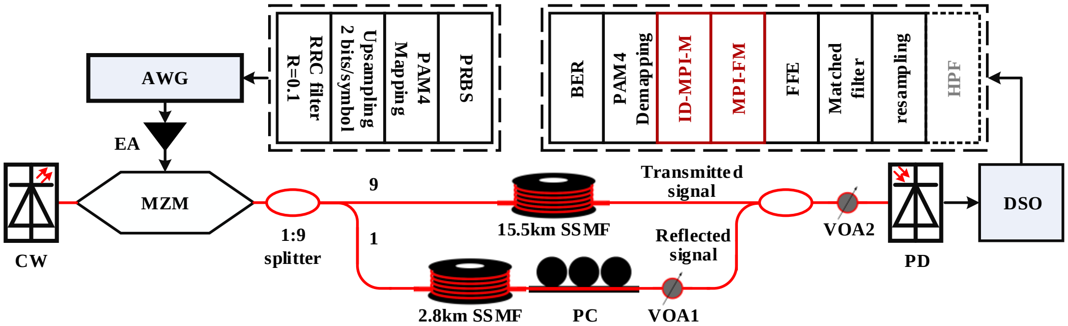

Fig. 2. Experimental setup of the MPI impaired IMDD PAM4 system.

cut-off frequency of 15MHz is used to suppress the MPI noise for comparison.

Fig. 3(a) and Fig. 3(b) show the results of bit error rate (BER) performance for a 100 kHz laser linewidth. It can be observed that the MPI-FM and ID-MPI-M algorithms both can effectively mitigate the MPI and improve the BER, and the HPF scheme is effective too. Besides, through the cascade of MPI-FM and ID-MPI-M algorithms, the BER performance can be further improved and the BER performance is better than that of the HPF scheme. With the help of MPI-FM and ID-MPI-M algorithms, the measured BER value of 56 Gb/s PAM4 signals can still reach the 7% HD-FEC limit when the SIR reaches 18 dB. Figs. 3(c-e) show the results of BER performance for a 4 MHz laser linewidth. It can be observed that the ID-MPI-M algorithm is still effective for large laser linewidth, but the HPF scheme is ineffective for larger laser linewidth and sometimes degrades the BER performance as shown in Fig. 3(e). Besides, the MPI-FM algorithm can slightly improve the BER performance, which could be attributed to the rapid fluctuation of the PAM4 signal caused by a large laser linewidth. However, through the cascade of MPI-FM and ID-MPI-M algorithms, the measured BER performance of 56 Gb/s PAM4 signals can be further improved, and a SIR tolerance of about 4 dB is achievable for large laser linewidth.

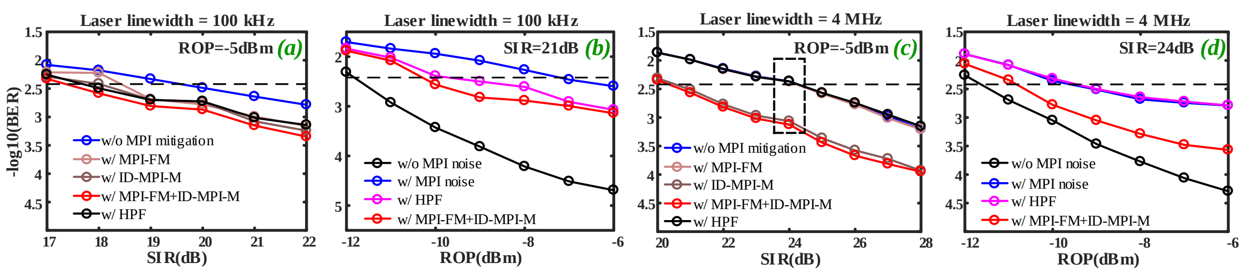

(e)	w/o MPI mitigation	w/ MPI-FM	w/ ID-MPI-M	w/ MPI-FM+ID-MPI-M	w/ HPF	Remark: laser linewidth=4MHz, SIR=24dB
BER	4.30e-3	4.20e-3	8.63e-4	7.51e-4	4.31e-3	

Fig. 3. The experiment results of 100 kHz laser linewidth, (a) BER versus SIR, (b) BER versus ROP when the SIR is 21 dB; and results of 4 MHz laser linewidth, (c) BER versus SIR, (d) BER versus ROP while the SIR is 24 dB, (e) BER performance of different conditions when SIR is 24 dB.

4. Conclusions

We propose two MPI noise mitigation algorithms for the IMDD PAM4 system, and successfully suppress the MPI noise in the Rx DSP for the first time. The MPI-FM and ID-MPI-M algorithms both can effectively suppress the MPI noise, and the cascade of MPI-FM and ID-MPI-M algorithm can further improve the system performance and performs better than the traditional HPF scheme. With the help of MPI-FM and ID-MPI-M algorithms, 56 Gb/s PAM4 signals after 15.5 km SSMF transmission is demonstrated under SIR of 18 dB, and a SIR tolerance of about 4 dB is achieved for a large laser linewidth of 4MHz.

5. Acknowledge

We thank the support of the National Key Research and Development Program of China (2018YFB1800904) and the National Nature Science Foundation of China (NSFC) (62171190).

6. References

[1] Man J, et al., in Proc. OFC, Paper M2E.7 (2014).
[2] Zhong K, et al., Opt. Express. 23, 1176-1189 (2015).
[3] Fludger C R S, et al., in Proc. OFC, Paper W1F.6(2014).
[4] Pepeljugoski P K, et al., J. Lightwave Technol. 10, 957-963 (1992).
[5] Wen Y J, et al, Opt. Express. 28, 38317-38333 (2020).
[6] Torres-Ferrera P, et al., J. Lightwave Technol. 38, 608-618 (2019).
[7] B. P. Smith, et al, U.S. Patent, US9876581B2.